MCAT Institute
Final Report
95-01

Development of an Upwind, Finite-Volume Code with Finite-Rate Chemistry

Gregory A. Molvik

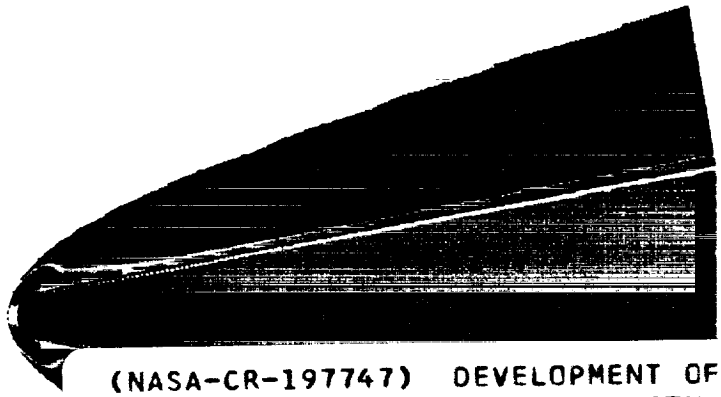

January 1995

NCC2-498

MCAT Institute
3933 Blue Gum Drive
San Jose, CA 95127

MCAT Institute

Development of an Upwind, Finite-Volume Code with Finite-Rate Chemistry

NCC2-498

Final Report

Period
August 1,1994 to January 31, 1995

Submitted to: NASA-Ames Research Center
Moffett Field, CA 94035
Dr. William R. Van Dalsem, Branch Chief
Dr. Scott L. Lawrence, Technical Monitor

Prepared by: MCAT Institute
3933 Blue Bum Drive
San Jose, CA 95127
Phone: (415)988-6514
Dr. Bala Balakrishnan, President
Dr. Gregory A. Molvik, Principal Investigator

ABSTRACT

Under this grant, two numerical algorithms were developed to predict the flow of viscous, hypersonic, chemically reacting gases over three-dimensional bodies. Both algorithms take advantage of the benefits of upwind differencing, total variation diminishing techniques and of a finite-volume framework, but obtain their solution in two separate manners. The first algorithm is a zonal, time-marching scheme, and is generally used to obtain solutions in the subsonic portions of the flow field. The second algorithm is a much less expensive, space-marching scheme and can be used for the computation of the larger, supersonic portion of the flow field. Both codes compute their interface fluxes with a temporal Riemann solver and the resulting schemes are made fully implicit including the chemical source terms and boundary conditions. Strong coupling is used between the fluid dynamic, chemical and turbulence equations. These codes have been validated on numerous hypersonic test cases and have provided excellent comparison with existing data. This report summarizes the research that took place from August 1,1994 to January 1, 1995.

This report summarizes the research that took place in the final six months of NASA Grant Number NCC2-498. It serves as the final report for this grant and constitutes the end product. The report preceding this report is MCAT Annual Report number 94-01.

FORWARD

In the six months associated with this report, two research objectives were addressed. The first was to enhance the capabilities of the TUFF code to include solid heat transfer effects. The second objective was to address propulsion-airframe integration (PAI) effects for the Reference-H, High-Speed Civil Transport (HSCT). Both of these efforts lasted three months each and the results are summarized in the two sections below.

Solid Heat Transfer Effects in TUFF

In periods preceding this report period, two numerical models were developed that contain many desirable features for the computation of three-dimensional, hypersonic flow fields. The first is a time-marching scheme. It is generally used to obtain the solution in the subsonic or separated regions of the hypersonic flow field. Extensive amounts of required computer time can prohibit the computation of an entire hypersonic flow field with a time-marching scheme of this nature. Hence, the second numerical scheme was developed. It is a space-marching scheme that obtains a solution in relatively little computer time and can be used to compute the larger supersonic portion of the flow field. The space-marching scheme has non-equilibrium, equilibrium and perfect gas capabilities and the time-marching scheme also has an incompressible option. Both codes employ a finite-volume philosophy to ensure that the schemes are fully conservative. Further, they obtain their upwind inviscid fluxes by employing a temporal Riemann solver that fully accounts for the gas model used. This property allows the flow field discontinuities such as shocks and contact surfaces to be captured by the numerical scheme without smearing. Total Variation Diminishing (TVD) techniques are included to allow extension of the schemes to higher orders of accuracy without introducing spurious oscillations. The schemes employ strong coupling between the fluid dynamic and species conservation equations and are made fully implicit to eliminate the step-size restriction of explicit schemes. This is necessary since step-sizes in a viscous, chemically reacting calculation can be excessively small for an explicit scheme, and the resulting computer times prohibitively large. A fully conservative zonal scheme has been implemented to allow solutions of very complex problems. The schemes are made implicit by fully linearizing all of the fluxes and source terms and by employing a modified Newton iteration to eliminate any linearization and approximate factorization error that might occur. Approximate factorization is then employed to avoid solving many enormous banded

matrices. Turbulence models include both zero and two equation models. Finally, a sublayer approximation is used in the space-marching algorithm to allow stable marching in the presence of a subsonic viscous layer. Validation of these codes includes comparison with exact, experimental and existing numerical results with very good success.

It was the first objective of this grant extension to further enhance the capabilities of the existing hypersonic codes. In particular, the TUFF code was coupled with a solid heat transfer code to more accurately predict wall temperatures and surface heat transfer. A finite-volume philosophy was maintained throughout this study to ensure conservation. Coupling of the two analysis procedures took place through the boundary conditions and was done explicitly. More details of this research are given in Appendix A of this report. Appendix A consists of an abstract to the AIAA 29th Thermophysics Conference entitled, "Computation of High-Speed Flow Fields with Multi-Dimensional Solid Heat Conduction." Because of the termination of this grant, this paper is expected to be presented by the second author, Dr. Frank S. Milos.

HSCT Propulsion/Airframe Integration

The second objective of this proposed research is the assessment of the performance of engine integrated high speed aircraft. In particular the effect of various Propulsion Airframe Integration(PAI) design variables on aerodynamic performance was addressed for the High-Speed Commercial Transport (HSCT) at critical conditions. The goal of this research was to obtain performance coefficients on various integrated configurations at these conditions to then be used in a vehicle synthesis code for aircraft design. These flight conditions that were addressed include 1) Subsonic Cruise, 2) Transonic conditions and 3) Supersonic Cruise. The base vehicle is the Reference-H configuration. Various parametric studies were computed to address the objective of this research. These cases are given below.

Individual Components - This case consists of the individual components at the three flight conditions. These components include the airframe, inboard nacelle and outboard nacelle. Each component was computed alone without any integration effects.

Nacelles Together - This case consists both the inboard and outboard nacelles run together at the three flight conditions. This case was included to predict the nacelle/nacelle interactions. These results show that the interaction is minimal.

Ref-H - This case consists of the baseline Reference-H integrated configuration at the three flight conditions. This case served as a reference for the parametric studies below.

Ref-H with 10% Larger Nacelles - This case consists of the Reference-H integrated configuration with 10% larger Nacelles at the three flight conditions.

Ref-H with Inboard Nacelle Moved Forward - This case consists of Reference-H integrated configuration with the inboard nacelle moved upstream 10% of the nacelle length. Again this geometry was run at the three flight conditions.

Ref-H with Inboard Nacelle Moved Backward - This case consists of Reference-H integrated configuration with the inboard nacelle moved downstream 5% of the nacelle length. Again this geometry was run at the three flight conditions.

A code search was performed at the beginning of this study to locate a Computational Fluid Dynamic code that was capable of predicting the flow field about an engine-integrated configuration. The AIRPLANE code was chosen for this study since computational grid files already existed for the Reference-H configuration. The AIRPLANE code is an inviscid, unstructured code with an automatic griding routine. It proved to be very simple to use and was ideal for this study. One shortfall was the unpredictable dependence of code convergence on the CFL number. This required experimentation to obtain an optimum number for all of the computations.

The computed surface pressure on the Reference-H at supersonic cruise conditions is shown in Figure 1. The flow field pressure in the vicinity of the inboard nacelle at all three flight conditions is shown for the baseline configuration in figures 2-4. The results for all of the cases are summarized in Table 1.

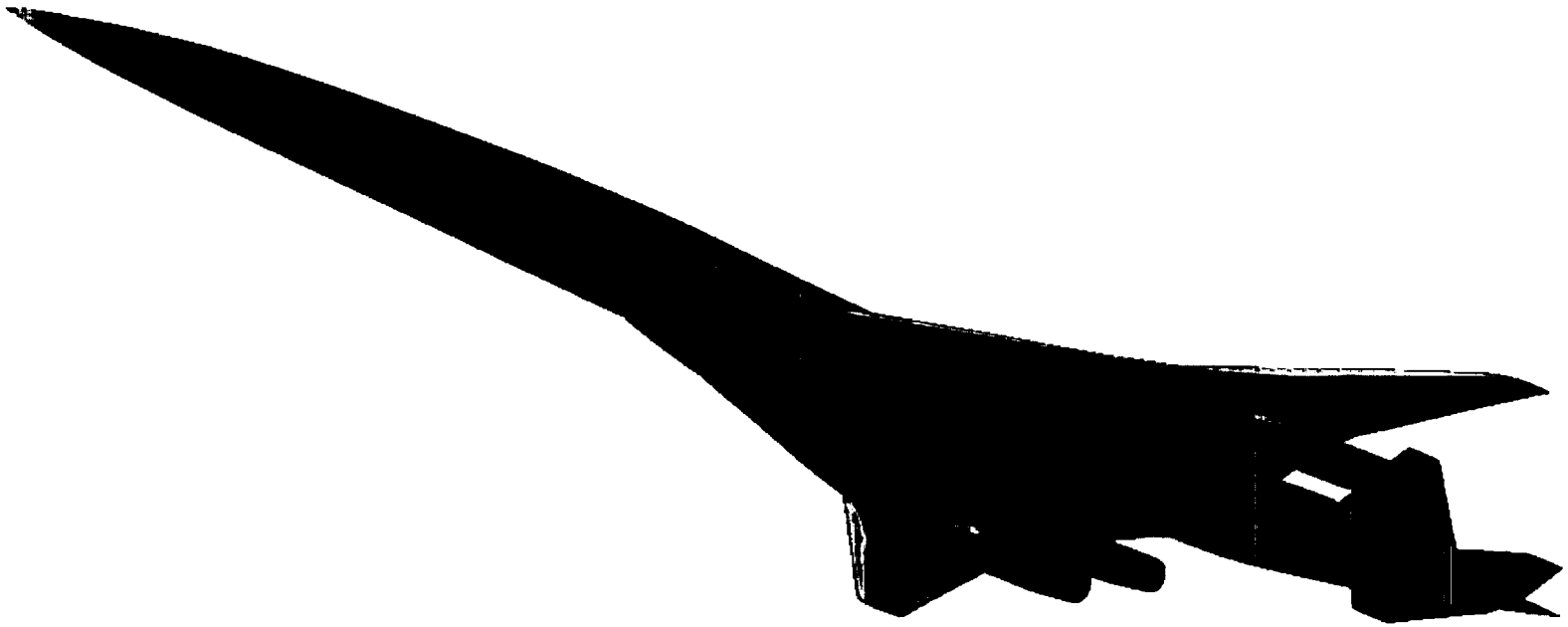

Figure 1. Pressure Contours on Reference-H Configuration

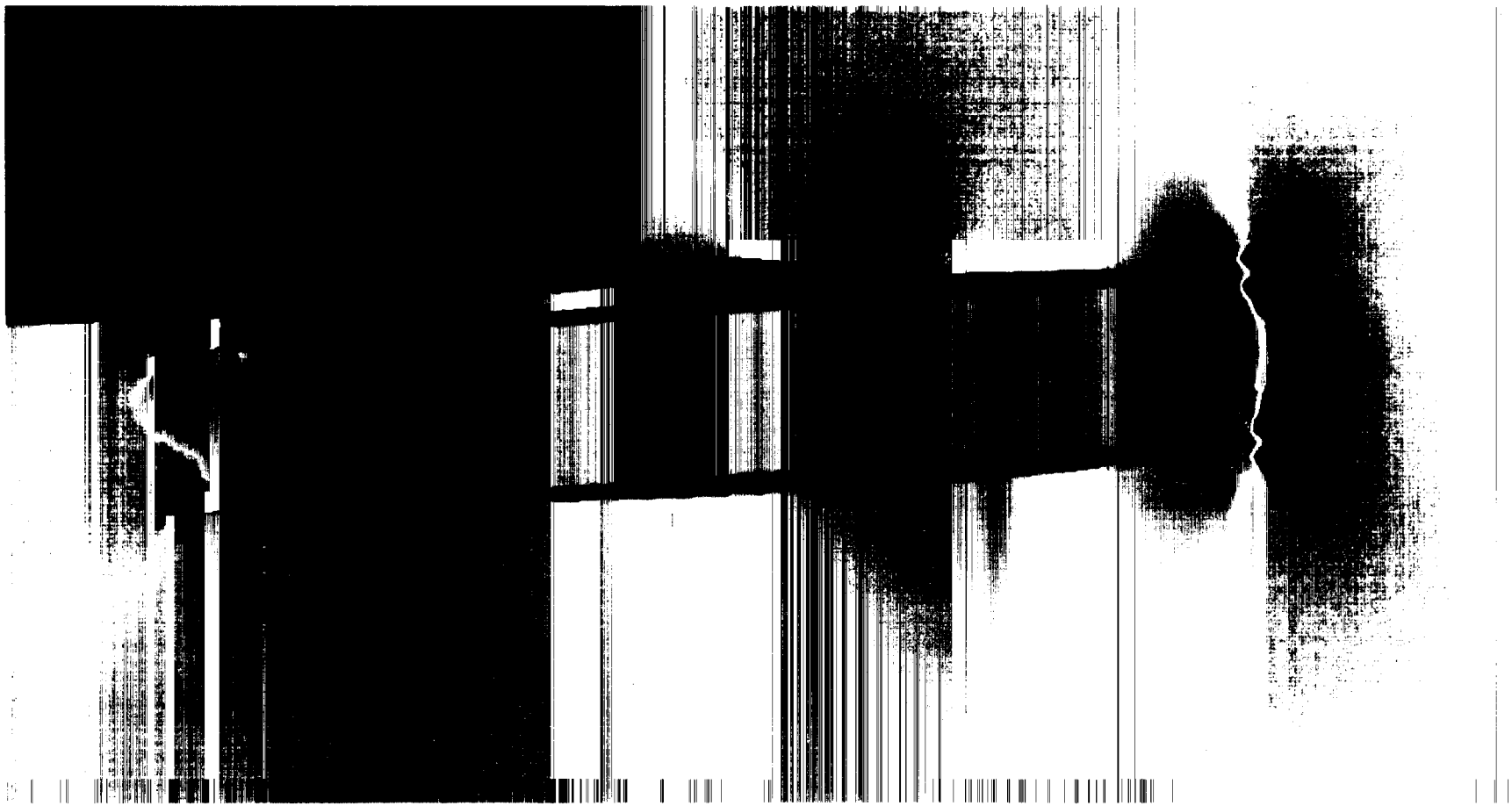

ORIGINAL PAGE
COLOR PHOTOGRAPH

Figure 2. Pressure Contours Near Nacelle (M=0.9)

Figure 3. Pressure Contours Near Nacelle (M=1.1)

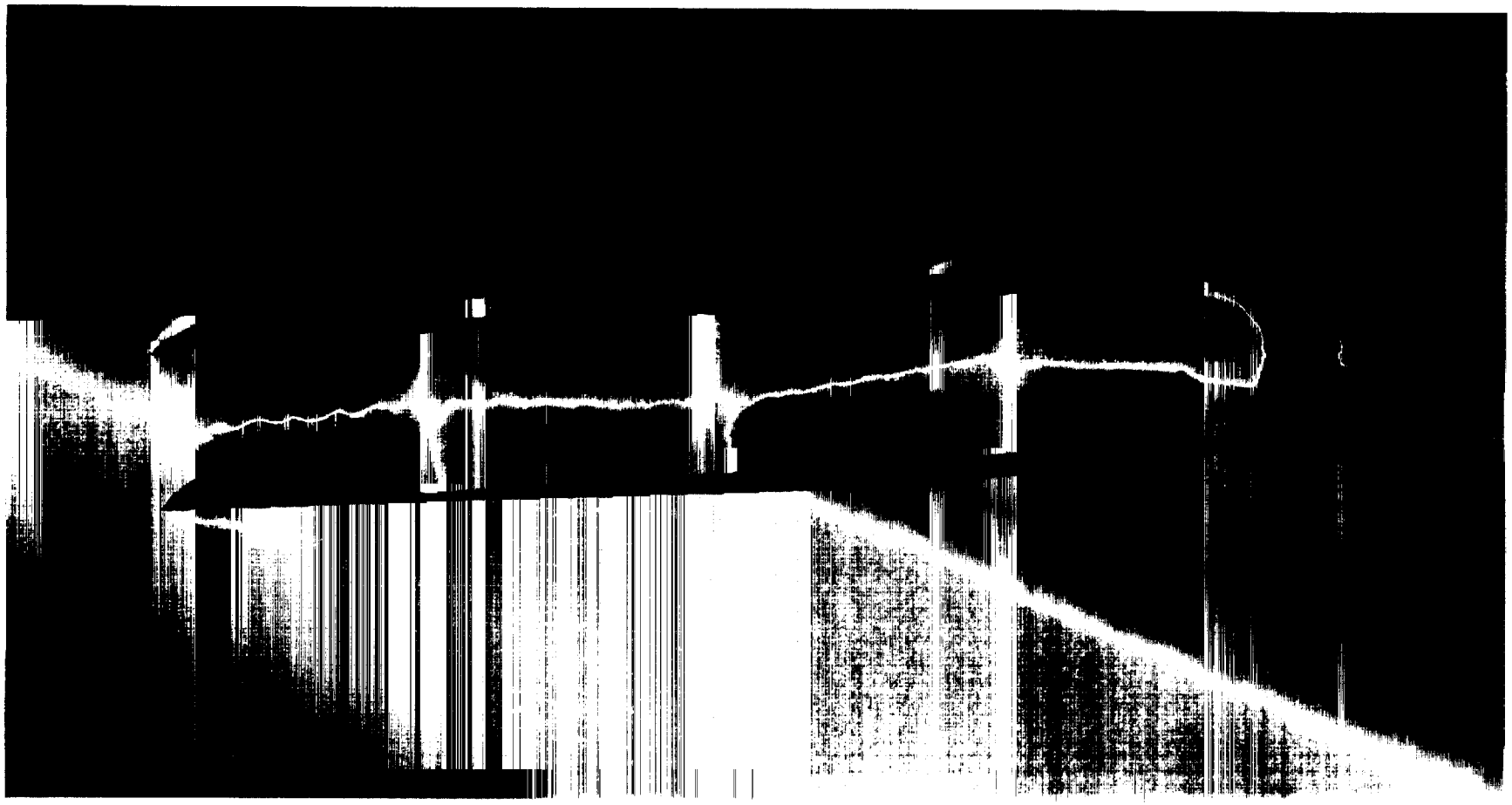

Figure 4. Pressure Contours Near Nacelle (M=2.4)

HSCT Reference H
Propulsion/Airframe Integration

Coefficients obtained with Airplane Code

Mach Number	0.90			1.10			2.40		
Alpha	5.70			2.87			3.80		
	Airplane	Inner Nacelle	Outer Nacelle	Airplane	Inner Nacelle	Outer Nacelle	Airplane	Inner Nacelle	Outer Nacelle
I.) Individual Components									
CL	0.281168	0.000634	0.001155	0.118648	-0.000523	0.000014	0.100862	-0.000139	0.000435
CD	0.020338	0.001007	0.001054	0.009123	0.001415	0.001418	0.008214	0.000375	0.000424
CM	-0.014122	-0.000453	-0.000564	-0.007838	-0.000233	-0.000366	-0.003592	-0.000062	-0.000228
CN	0.281798	0.000730	0.001254	0.118956	-0.000452	0.000085	0.101184	-0.000114	0.000462
CA	-0.007688	0.000939	0.000934	0.003171	0.001439	0.001416	0.001511	0.000383	0.000394
II.) Nacelles Only									
CL	-	0.000722	0.001194	-	-0.000506	-0.000045	-	-0.000131	0.000479
CD	-	0.000968	0.001149	-	0.001510	0.001504	-	0.000354	0.000377
CM	-	-0.000471	-0.000591	-	-0.000271	-0.000352	-	-0.000061	-0.000242
CN	-	0.000814	0.001302	-	-0.000429	0.000031	-	-0.000107	0.000502
CA	-	0.000892	0.001024	-	0.001533	0.001504	-	0.000362	0.000344
III.) Standard Airplane									
CL	0.300820	-0.001730	-0.000249	0.142731	-0.001798	-0.000145	0.107188	-0.000249	0.000951
CD	0.022686	0.000633	0.000808	0.009278	0.001172	0.001294	0.008352	0.000336	0.000554
CM	-0.017875	0.000639	-0.000042	-0.015575	0.000582	-0.000240	-0.006664	-0.000161	-0.000760
CN	0.301585	-0.001658	-0.000168	0.143017	-0.001737	-0.000080	0.107506	-0.000226	0.000986
CA	-0.007304	0.000801	0.000829	0.002120	0.001261	0.001300	0.001230	0.000352	0.000490

Table 1. PAI Coefficients

HSCT Reference H
Propulsion/Airframe Integration

Coefficients obtained with Airplane Code

Mach Number	0.90			1.10			2.40		
Alpha	5.70			2.87			3.80		
	Airplane	Inner Nacelle	Outer Nacelle	Airplane	Inner Nacelle	Outer Nacelle	Airplane	Inner Nacelle	Outer Nacelle
IV.) Airplane with 10% Larger Engines									
CL	0.300989	-0.002033	-0.000239	0.144280	-0.002060	-0.000181	0.107767	-0.000703	0.000822
CD	0.022794	0.000667	0.000870	0.009321	0.001317	0.001441	0.008350	0.000383	0.000608
CM	-0.017757	0.000767	-0.000059	-0.015841	0.000661	-0.000267	-0.006815	0.000042	-0.000739
CN	0.301764	-0.001957	-0.000152	0.144566	-0.001991	-0.000109	0.108083	-0.000676	0.000861
CA	-0.007213	0.000866	0.000889	0.002085	0.001418	0.001449	0.001190	0.000429	0.000553
V.) Airplane Inboard Nacelle Moved Forward									
CL	0.292506	-0.000935	-0.000277	0.142017	-0.001027	-0.000267	0.107560	0.000108	0.000960
CD	0.022327	0.000419	0.000711	0.009519	0.001155	0.001341	0.008371	0.000378	0.000554
CM	-0.015309	0.000297	0.000005	-0.014594	0.000161	-0.000178	-0.006644	-0.000450	-0.000769
CN	0.293277	-0.000889	-0.000205	0.142315	-0.000968	-0.000199	0.107878	0.000133	0.000995
CA	-0.006835	0.000510	0.000735	0.002397	0.001205	0.001353	0.001224	0.000370	0.000489
VI.) Airplane Inboard Nacelle Moved Backward									
CL	0.302283	-0.001891	-0.000236	0.142032	-0.001991	-0.000113	0.106856	-0.000356	0.000943
CD	0.022670	0.000742	0.000845	0.009175	0.001212	0.001251	0.008353	0.000329	0.000560
CM	-0.018375	0.000696	-0.000058	-0.015619	0.000689	-0.000250	-0.006573	-0.000061	-0.000756
CN	0.303040	-0.001808	-0.000151	0.142314	-0.001928	-0.000050	0.107175	-0.000334	0.000978
CA	-0.007465	0.000926	0.000864	0.002052	0.001310	0.001255	0.001253	0.000352	0.000496

Table 1. PAI Coefficients

Appendix I

Abstract for the AIAA 29th Thermophysics Conference

Computation of High-Speed Flow Fields
with Multi-Dimensional Solid Heat Conduction

Abstract for the AIAA 29th Thermophysics Conference to be held on June 19-22, 1995 at San Diego, CA.
Abstract Deadline: October 17, 1994.

Computation of High-Speed Flow Fields with Multi-Dimensional Solid Heat Conduction

Gregory A. Molvik†, Frank S. Milos‡, Thomas H. Squire* and Yih-Kano Chen*
NASA Ames Research Center
Moffett Field, CA 94035

ABSTRACT

In this paper, two methods are presented for the computation of high-speed flow fields that account for heat transfer to and within a vehicle. Emphasis is placed on the modeling of a material composed of a diboride composite. The first method couples a heat conduction computation with a hypersonic boundary layer code through manual iteration. The second approach is a more comprehensive method that employs a surface energy balance to couple a new finite-volume, multi-dimensional, heat transfer code with a hypersonic computational fluid dynamic code. Generalized coordinate transformation are employed in both the fluid and solid solvers, and the flow field solution and the vehicle thermal response are obtained simultaneously. This approach allows the computation of time-accurate, transient behavior. A finite-volume philosophy is maintained in both models to ensure conservation of energy. Results are obtained for a simple conduction problem and on a blunt wedge geometry at hypersonic speeds. The final version of this paper will also include a three-dimensional transient computation of a hypersonic test problem.

INTRODUCTION

The TPS/structural weight of hypersonic vehicles and spacecraft is typically much larger than the payload weight. For this reason any improvement in the fidelity of TPS sizing calculations which leads to an actual reduction in TPS weight has a significant cost and feasibility impact on vehicle design[1]

To reduce uncertainties in TPS sizing, efforts to couple material response with CFD calculations have proceeded rapidly in the last two years. Initial work suggested the coupling of semi-analytic, approximate heat-conduction models and surface energy and mass balances with CFD codes[1]. Recent efforts have demonstrated that finite difference and finite volume thermal solvers can be used to calculate heat conduction into the vehicle TPS [2-3]. This work presents the results of two analysis techniques that couple a flow field solver with a thermal response model.

The Thermal Protection Branch at NASA Ames has developed diboride composites[4], which when heated in air, develops a thin, adherent, high-melting-point oxide coating. These diboride composites are candidate materials for high heat flux areas of hypersonic vehicles and spacecraft where other materials could not survive without some type of active cooling. The primary application of the diboride materials is as reusable nosetips and wing leading edges.

To predict the performance of these materials in this application, it is necessary to perform calculations which include multidimensional solid heat conduction coupled with the flow field. This is the focus of this paper.

ANALYSIS TOOLS

Two methods of analysis are presented in this study. The first technique manually couples a boundary layer code with a heat transfer code. The second technique is a more comprehensive model that uses a surface energy balance to couple a hypersonic CFD code with a fully compatible heat transfer code.

COSMOS/BLIMP

---

† Senior Research Scientist, MCAT Institute, Member AIAA

‡ Aerospace Engineer, Thermal Protection Branch

* Research Scientists, Thermosciences Institute at NASA Ames, Members AIAA

The first method couples two existing codes, BLIMP and COSMOS and requires a manual iteration between them. BLIMP[5-6] is a reacting hypersonic boundary layer code which includes multispecies diffusion and transport properties, chemical reactions or chemical equilibrium, and numerous options for boundary-layer edge and surface boundary conditions. COSMOS[7] is general-purpose finite element software for computing material thermal and structural response.

The procedure begins with surface pressure and boundary layer edge conditions from an Navier Stokes flow solution. A BLIMP calculation using radiative equilibrium at the wall finds an initial guess for the local wall temperature T_w. The detailed BLIMP solution also provides estimates of the parameters h and T_∞ for use in the COSMOS convective heat-transfer boundary condition:

$$q_w^{BLIMP} = h(T_\infty - T_w) = \sigma\varepsilon T_w^4 - q_{cond}$$

The COSMOS code is time-marched to steady state to find the temperature distribution in the solid and, in particular, the conduction-corrected value of T_w BLIMP is then re-run with the prescribed wall temperature to find updated values for the coefficients h and T_∞. Several iterations between BLIMP and COSMOS were required to reach self-consistent values for h, T_w, and T_∞.

The high-temperature catalycity of the diboride materials has not yet been measured. To bound the range of possible surface conditions, two options were used for chemistry in the BLIMP calculations. One option, equilibrium air chemistry, provides a good approximation for a fully catalytic surface. The other option, 5-species finite-rate air chemistry[8] with no surface reactions, approximates a non-catalytic surface.

TUFF-HT

Computational fluid dynamics has and will continue to play an important role in the design and analysis of hypersonic systems. This is true because ground based facilities are expensive to operate and in many cases cannot duplicate the exact flight conditions of such vehicles. Requirements of a numerical algorithm are very demanding for hypersonic computations. The algorithm must be capable of predicting the three-dimensional flow of a highly turbulent mixture of reacting gasses with separated regions and strong flow field discontinuities. Multi-equation turbulence models become a requirement to accurately compute the numerous shear layers and boundary layers that are present. Further, upwind algorithms offer an appealing approach to solutions of hypersonic flow fields because of the ability to capture strong flow field discontinuities without user-specified smoothing terms. A strongly coupled, non-equilibrium chemistry model is required to compute the highly reactive flow fields typical of high speed flight. Finally, the solver must account for the heat transfer to and within the vehicle to accurately predict surface temperatures and net heat fluxes to a vehicle.

For the present CFD analysis, the TUFF code of Ref. 9 was chosen since it contains many of the desired features required for hypersonic computations. The TUFF code is a time-marching code that contains nonequilibrium, equilibrium, perfect and incompressible gas models. It employs a finite-volume philosophy to ensure that the scheme (including the boundary conditions) is fully conservative. Further, it obtains its upwind inviscid fluxes by employing a Riemann solver that fully accounts for the gas model used. This property allows the flow field discontinuities, such as shocks and shear layers, to be captured without significant amounts of smearing. Total variation diminishing (TVD) techniques are included to allow extension to higher orders of accuracy without introducing spurious oscillations. The scheme employs a strong coupling between the fluid dynamic and chemistry equations which are made fully implicit to eliminate the step-size restriction of explicit schemes. A fully conservative zonal scheme[10] has been implemented to allow solutions of geometrically complex problems. Turbulence models include both a zero[11] and two-equation [12] model with a correction for compressibility [13].

In the final version of this paper, details of the new heat transfer code and the coupling procedure will be presented here. It should be noted for this abstract that a single code containing both the fluids solver, TUFF, and a new finite-volume heat transfer solver was generated. Any interface between two zones, independent of the solver used in each, is triangulated using an unstructured technique similar to that of Reference 10.

Coupling between the fluid zone and a solid zone takes place with the following surface energy balance(SEB).

$$\underbrace{\kappa \frac{\partial T}{\partial n} + \rho D \sum_s h_s \frac{\partial c_s}{\partial n}}_{Fluid} - \underbrace{\kappa \frac{\partial T}{\partial n}}_{Solid} - \underbrace{\varepsilon \sigma T_w^4}_{Surface} = 0$$

This SEB is employed on the interface in both the fluid and solid zones and it uses the latest known information from the other zone. The surface temperature is determined with this SEB. An interface between two solid zones is simply a match of two heat flux terms at the interface.

RESULTS

There are three test cases included in this paper. The first is a simple conduction problem that serves as a test case for the new heat transfer code in TUFF. The second test case is that of a wing leading edge to determine the survivability of a diboride composite exposed to hypersonic conditions and to compare the two analysis procedures. A third test case to be included in the final version of this paper is a hypersonic projectile validation case. This case will demonstrate the three-dimensional, transient capability of the TUFF code and also will serve as a validation case. Experimental results will be compared to the predicted values where possible.

Simple Conduction Problem

The first test case for the new finite-volume heat transfer module of the TUFF code is a simple heat conduction problem. It consists of a square piece of a material with constant conductivity Two opposite sides are adiabatic and two sides are held at two different temperatures. The analytic solution to this problem at the steady state is a constant temperature gradient throughout the materiel. The grid for this test case is shown in Fig. 1 and was generated unconventionally to test the numerical scheme and to ensure that the exact solution is obtained even on non-orthogonal grids.

The TUFF heat transfer solution is shown in Fig. 2. Evenly spaced, vertical temperature contours indicate that the exact solution is indeed obtained. In contrast, Fig. 3 shows a solution with the same method but neglects the thermal cross-derivative terms mentioned above. Even though these cross-derivative terms are small compared with the total heat flux, this erroneous result clearly demonstrates the importance of incorporating these terms in a finite-volume heat transfer code.

Blunt Wing Leading Edge

The second test case is that of a two-dimensional wing leading edge exposed to hypersonic conditions. The material is a diboride composite (ZrB_2 + SiC) with a nose radius of 0.1in and a 5 degree half-angle. The emmisivity, ε, is assumed to be 0.6. The length of the geometry is 3.19in. The flow medium is air and the flow conditions are listed below.

M = 15
Altitude = 100kft.

Both a TUFF solution and a COSMOS/BLIMP solution were obtained for this test case. It was assumed that the base of the wing leading edge was adiabatic for these computations. The grid (every fourth grid line) used in the TUFF calculation is shown in Figure 4. Both the fluid and solid grids measured 80x55x2. The grid used in the COSMOS/BLIMP runs is of similar dimensions.

Figures 5 shows the TUFF predicted pressure contours contours . The pressure contours were virtually unchanged with the inclusion of the solid conduction model. The temperature are shown in Fig. 6 and 7 for the adiabatic and conducting solid cases. There is clearly an impact on the boundary layer temperature profiles when solid conduction is included. The solid temperature contours in the conducting case depict a thermal gradients that indicate a positive heat flux to the geometry in the nose region and a negative heat flux in the aft region.

In these results, the rearward-facing diboride surface was assumed to be insulated; i.e., thermally isolated for the rest of the wing. Under these conditions at steady state there is zero net heat flux into the wing tip. Heat absorbed near the stagnation point is conducted through the material to downstream locations where it is radiated from the surface. This effect is similar to that seen in heat-pipe-cooled components except that now the diboride solid itself takes the place of the heat-pipe working fluid. This effect is seen in the TUFF results of Figure 8 with lower nose temperature and higher aft temperatures when solid conduction is included. A good comparison of nose temperatures is seen between the two methods however they begin to depart further down stream. The cause of this

discrepancy will be addressed in the final version of this paper.

One scenario which was investigated is hypersonic cruise conditions where the goal is to calculate the maximum wing leading edge temperature as a function of altitude and vehicle Mach number. Figure 9 shows the stagnation point temperature as a function of Mach number for two cases which provide upper and lower bounds for the surface catalyticity effects. The upper curve for a fully catalytic surface provides a conservative estimate of the surface temperature. Using 4000 F (2477 K) as the as the maximum use temperature, it can be seen that this material and geometry can operate up to a Mach number of 10.8 at 100kft. If the material is found to have low catalytic, the lower curve is appropriate and the configuration may operate up to a Mach number of 12.5.

Three Dimensional Transient Test Case

...to be included in the final version of this paper.

ACKNOWLEDGMENTS

This work was partially supported by NASA Ames Research Center under grants NCC2-498 and NAS2-14031.

REFERENCES

[1] Milos, F.S., and Rasky, D.J., "Review of Numerical Procedures for Computational Surface Thermochemistry," J. Spacecraft and Rockets, Vol. 8, No. 1, 1994, pp. 24-34.

[2] Keenan, J.A., and Candler, G.V., "Simulation of Graphite Sublimation and Oxidation under Re-Entry Conditions," paper AIAA 94-2083, June 1994.

[3] Chen, Y.K., Henline, W.D., and Tauber, M.E., "Trajectory Based Heating and Ablation Calculations for Mars Pathfinder Aeroshell," submitted to J. Spacecraft and Rockets, 1994.

[4] Bull, J.D., and Rasky, J.D., "Stability Characterization of Diboride Composites Under High Velocity Atmospheric Flight Conditions," Proceedings of the 24th International SAMPE Technical Conference, Oct. 20-22, 1992, T-1092.

[5] Bartlett, E.P., and Kendall, R.M., "An Analysis of the Chemically Reacting Boundary Layer and Charring Ablator. Part III: Nonsimilar Solution of the Multicomponent Laminar Boundary Layer by an Integral Matrix Method," NASA CR-1062, June 1968.

[6] Kendall, R.M., and Anderson, L.W., "Nonsimilar Solutions for Laminar and Turbulent Boundary-Layer Flows over Ablating Surfaces," AIAA Journal, Vol. 10, No. 9, 1972, pp. 1230-1236.

[7] Lashkari, M., "COSMOS/M User Guide, Volume 1, "Structural Research and Analysis Corp., Santa Monica, CA, April 1992.

[8] Dunn, M.G., and Kang, S.-W., "Theoretical and Experimental Studies of Reentry Plasmas," NASA CR-2232, April 1973.

[9] Molvik, G. A. and Merkle, C. L., "A Set of Strongly- Coupled Upwind Algorithms for Computing Flows in Chemical Nonequilibrium," AIAA Paper 89-0199. Jan. 1989.

[10] Klopfer, G. H. and Molvik G. A., "Conservative Multizonal Interface Algorithm for the 3-D Navier-Stokes Equations," AIAA Paper 91-1601, June 1991.

[11] Baldwin, B. S. and Lomax, H., "Thin Layer Approximation and Algebraic Model for Separated Turbulent Flows." AIAA Paper 78-257, Jan. 1978.

[12 Jones, W. P. and Launder, B. E., "The Prediction of Laminarization with a Two-Equation Model of Turbulence," *International Journal of Heat and Mass Transfer*, Vol. 15, 1972, pp. 303-314.

[13] Zeman, O., "Compressible Turbulence Subjected to Shear and Rapid Compression," Eighth Symposium on Turbulent Shear Flows, Munich, Germany, Sept, 1991.

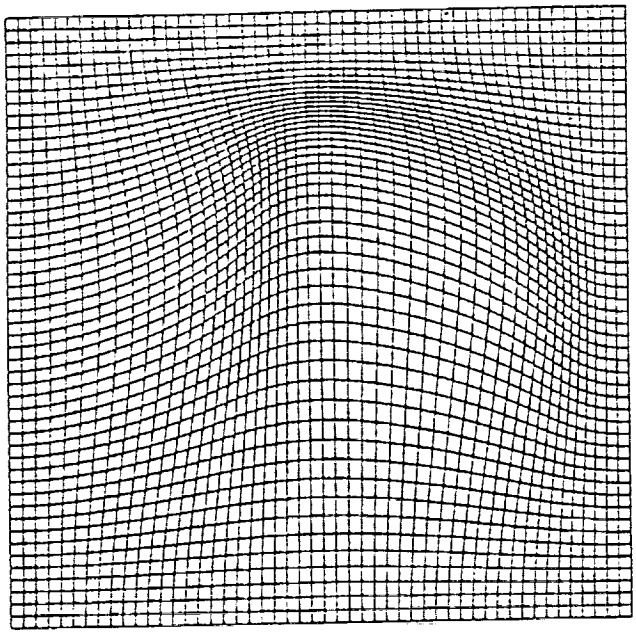

Fig. 1 Heat Transfer Grid for Simple Conduction Problem

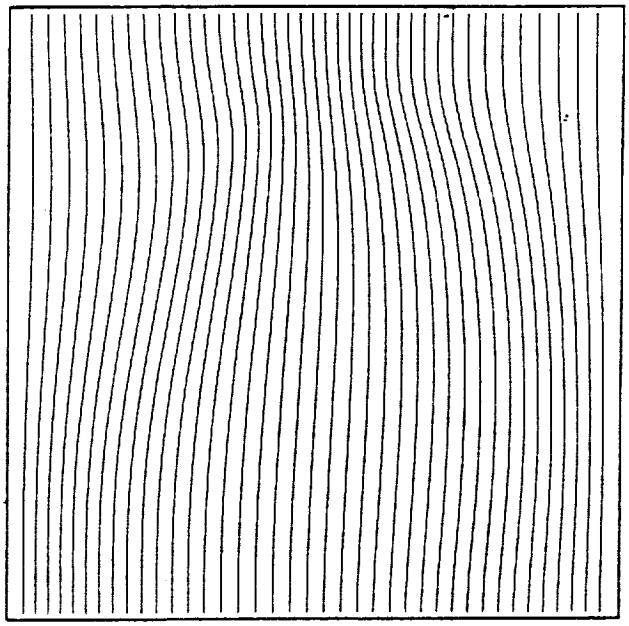

Fig. 3 Temperature Contours for Simple Conduction Problem without Cross Derivatives

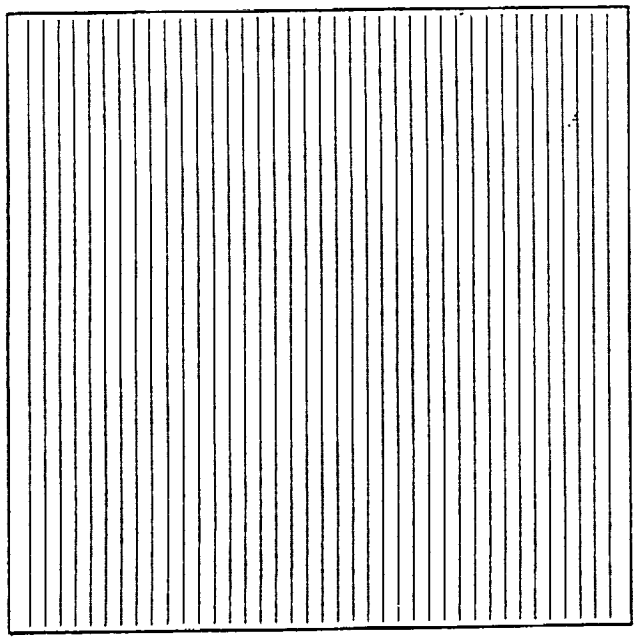

Fig. 2 Temperature Contours for Simple Conduction Problem

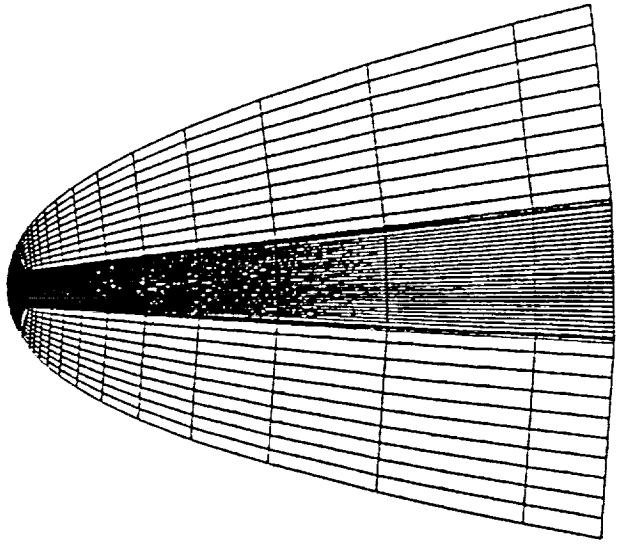

Fig. 4 TUFF Grids for Blunt Wing Test Case

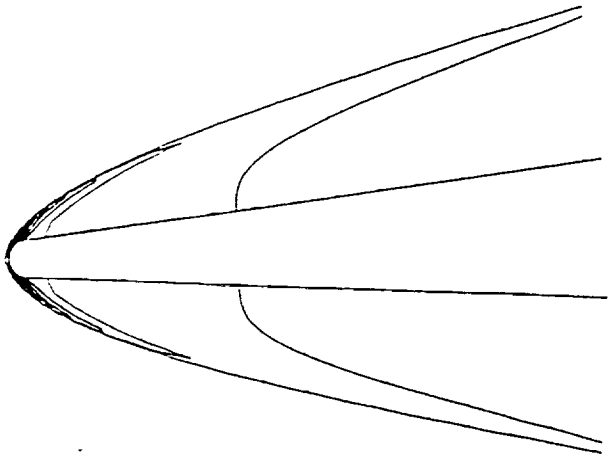

Fig. 5 TUFF Pressure Contours for Blunt Wing Test Cases

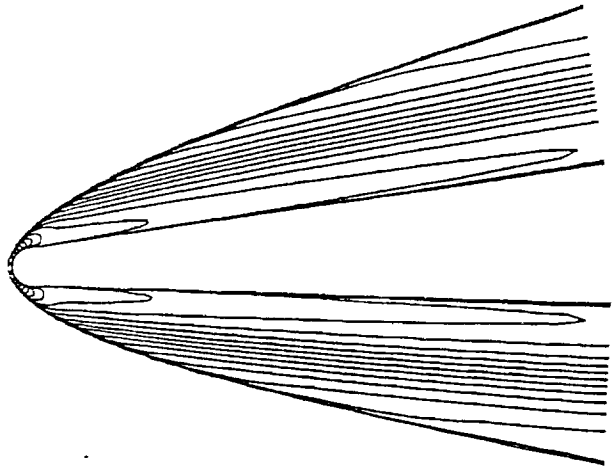

Fig. 7 TUFF Temperature Contours for Blunt Wing Test Case (with out Solid Conduction)

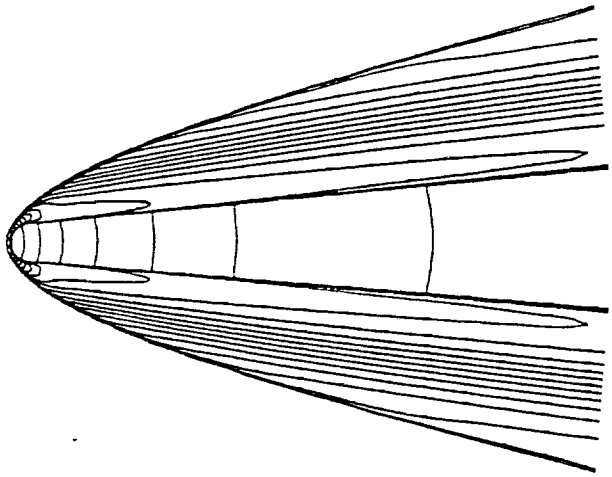

Fig. 6 TUFF Temperature Contours for Blunt Wing Test Case (with Solid Conduction)

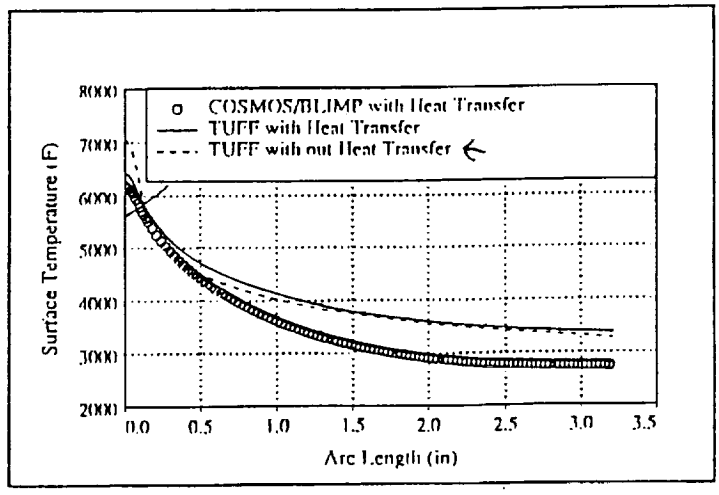

Fig. 8 Surface Temperature for Blunt Wing Test Case

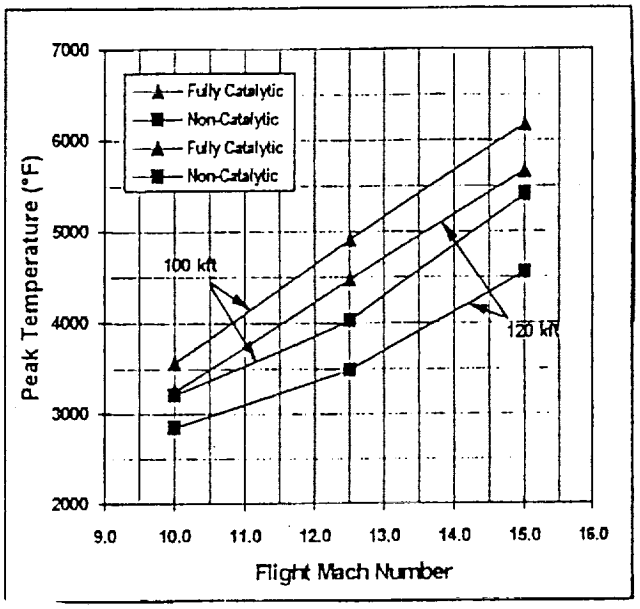

Fig. 9 Maximum Temperature vs. Mach No. for Blunt Wing Test Case